FROM RESEARCH TO INDUSTRY

MODELING PHASE SEPARATION IN THE MELT: THERMODYNAMICS, FLUID FLOW AND HPC SIMULATIONS

September 27th, 2023

A. Cartalade[a], W. Verdier[a], C. Méjanès[a], S. Schuller[b], S. Gossé[c], R. Le Tellier[d]

[a]CEA – Paris-Saclay, ISAS, DM2S, STMF, LMSF
[b]CEA – Marcoule, ISEC, DPME
[c]CEA – Paris-Saclay, ISAS
[d]CEA – Cadarache, IRESNE, DTN, SMTA, LMAG

Outline

1. Introduction: demixing in nuclear glass
2. Simulations of thermodynamics
3. 3D simulations of thermo with fluid flow
4. Current works – Perspectives
5. Appendices

Outline

Introduction: demixing in glass

Observations of phenomena in glass (CEA/DPME)

Intermediate temperature

Crystal growth

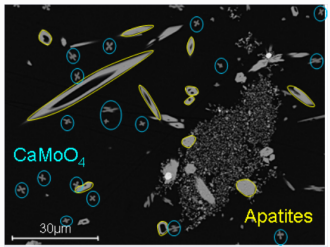

E. Régnier (DPME, 2011)

Phase separation of 2 liquids (high temperature)

Nucleation–growth

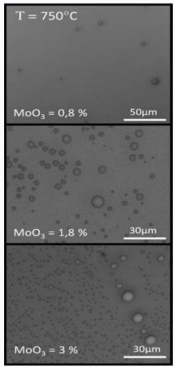

S. Schuller (DMPE, 2012)

Spinodal decomposition

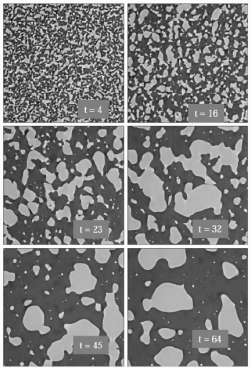

D. Bouttes (PhD 2013)

Thermodynamics of both demixing regimes

Concept

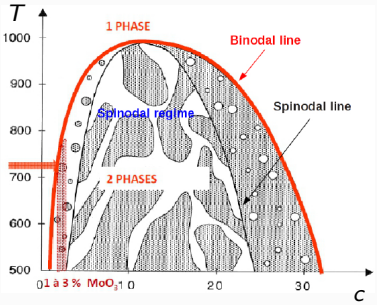

- Homogeneous mixture of SiO_2 and MoO_3 for $T > T_c$ (T_c critical temperature)
- For $T < T_c$ the system is unstable; SiO_2 and MoO_3 start to separate.

Phase diagrams of SiO_2–MoO_3 (2 phases + 2 comp)

Observation

S. Schuller (DPME, 2013)

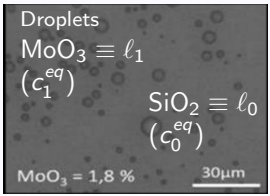

Binary phase diagram

From S. Gossé, (DRMP, 2013)

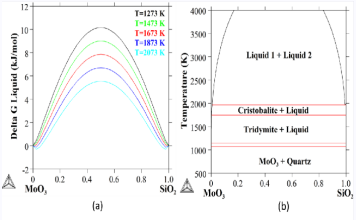

The "composition" $c(\boldsymbol{x}, t)$ is defined such as locally

$$c_1^{eq} \leq c(\boldsymbol{x}, t) \leq c_0^{eq}$$

Notations:

- ^{eq} for thermo equilibrium
- 0 for "Matrix" and 1 for "Droplets"

Phase diagrams for SiO_2–Na_2O–MoO_3

Calphad modeling from S. Gossé

Thermodynamics of three components

Gibbs triangle

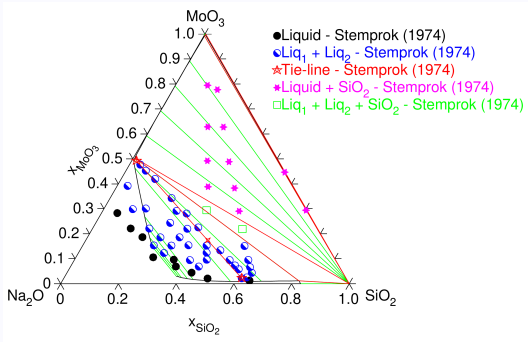

From S. Bordier (PhD, 2015)

T-*c* phase diagram

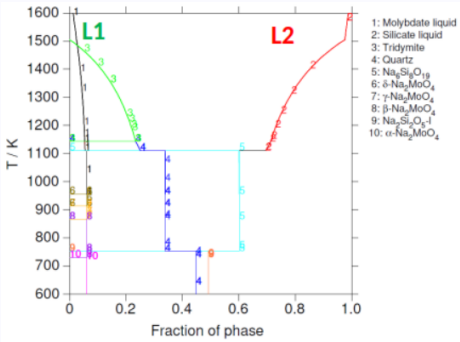

From S. Gossé & S. Schuller (2023)

Objectives of this presentation

For simulating phase separation

- What are the math equations ? Part 2
- How to connect them with the thermo database of Calphad modeling ? Part 2
- How to take into account the effects of viscosity and density (gravity) ? Part 3

Math model based on the "phase-field theory"

Advantages

- Thermodynamic consistency
- Interface-tracking (eulerian approach with diffuse interface)
- Possible expansion for 3-phases and n-components

Drawbacks

- ▸ Appendix

Methodology presented for simplified glass

- For two components: SiO_2 – MoO_3 (binary)
- For three components: SiO_2 – Na_2O – MoO_3 (ternary)
- For constant temperature

Overview of the phase-field theory

Concepts of phase-field method

- Introduction of a *phase-field* $\phi(\boldsymbol{x}, t)$
- Its evolution minimizes a *thermodynamic potential*

  ex. *free energy* $\mathscr{F}[\phi, c]$ (or *grand pot*, *Gibbs*, ...)

$$\mathscr{F}[\phi, c] = \int_V \left[H f_{dw}(\phi) + \frac{\zeta}{2}(\boldsymbol{\nabla}\phi)^2 + f_{bulk}(\phi, c) \right] dV$$

- Coupled to balance Eqs (mass, impulsion, ...)

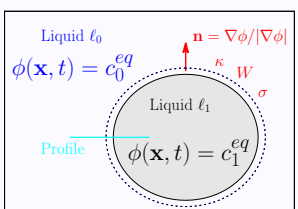

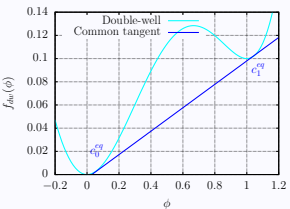

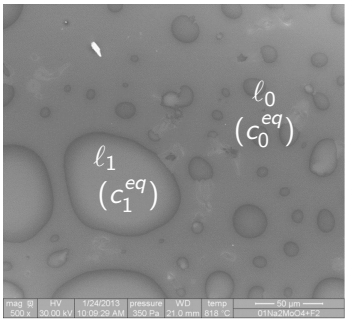

Interface nomenclature

- W interface width
- σ surface tension
- $\boldsymbol{n}(\boldsymbol{x}, t)$ unit normal vector
- $\kappa(\boldsymbol{x}, t)$ curvature $(= \boldsymbol{\nabla} \cdot \boldsymbol{n})$

Methodology of phase-field simulations

From experiments (DPC, DE2D, ...)

Phase-field models (ϕ-models)

- Assumptions
- Derive PDEs

ϕ-models+LBM

- PhD
- List of pheno

Lattice Boltzmann Methods

- Writing numerical schemes
- C++ implementation
- HPC simuls (part 3)

This presentation

Crystal growth & flow (2015)

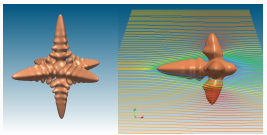

SIVIT project

Porous media dissolution (2022)

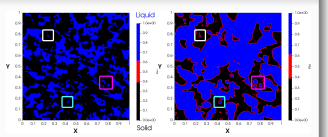

VESTA project

Liquid/gas phase change (2020)

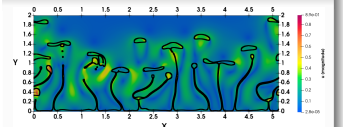

SITHY project

Binary/ternary demixing

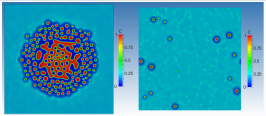

SIVIT project

Buoyancy & R-T instability

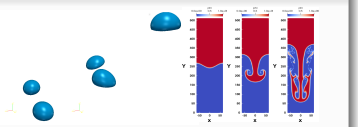

- List of pheno

RBNEW project

Simulations of thermodynamics

Two-phase with two components: Cahn-Hilliard model

Cahn-Hilliard with advection (mass balance+flux $j_{CH} = -M_\phi \nabla \mu_\phi$)

$$\frac{\partial \phi}{\partial t} + \overbrace{\nabla \cdot (\phi \boldsymbol{u})}^{\text{Advective term}} = \overbrace{M_\phi \nabla^2 \mu_\phi}^{\text{Diffusive term}}$$

$$\mu_\phi = 1.5\sigma \Big[\underbrace{16\phi(1-\phi)(1-2\phi)/W}_{\text{double-well derivative}} - W\nabla^2\phi \Big]$$

ϕ plays two roles: interface tracking and composition

Average compositions

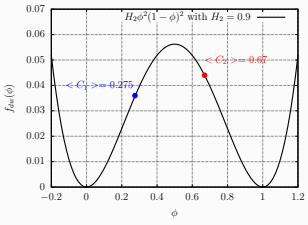

Simulations (with $u = 0$)

Spinodal decomposition with surfactant

Appendix

Nucleation and growth

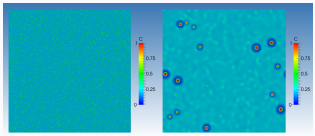

Video

Phase sep with gaussian distrib

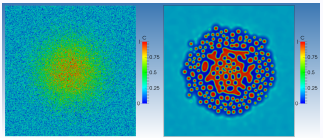

Video

Demixing $\langle C_1 \rangle = 0.275$, $\langle C_2 \rangle = 0.67$

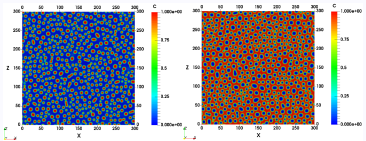

Video

Pros and cons of Cahn-Hilliard model

1. Advantages

1. Simulates various phenomena:
   - droplets coalescence, R-Taylor instab
   - spinodal decomposition
   - etc ...
2. Can be extended to 3 components

2. Drawbacks

1. Fourth-order derivative (bi-laplacian)
2. Contains the thermodynamics and the interface properties

→ difficult to fit thermodynamic without modifying σ and W

3. Need of alternative model

Separate "interface" and "diffusion" properties for 2 phases and multi-components system

↓

model based on the Allen-Cahn equation (example on 3 components)

Two-phase with three components SiO_2–Na_2O–MoO_3

Phase diagram with Calphad modeling

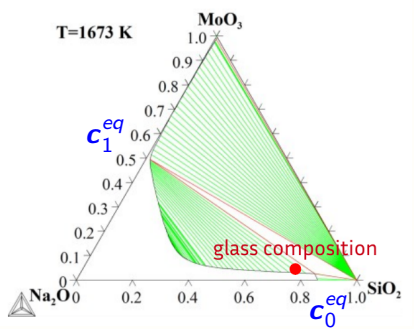

Ternary glass equilibrium

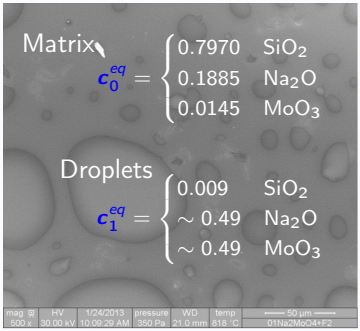

Three compositions (at 1152°C) for each oxyde:

SiO_2	: 78.79%	(C^A)
Na_2O	: 19.21%	(C^B)
MoO_3	: 2%	$(1 - C^A - C^B)$

Notations

$$\boldsymbol{C}^{glass} = (C^A, C^B)$$

$$\boldsymbol{c}_\Phi^{eq} = (c_\Phi^{A,eq}, c_\Phi^{B,eq})$$

Grand-potential formulation of phase-field model

Use $\boldsymbol{\mu} = (\mu_A, \mu_B)$ for defining the thermodynamics (not $\boldsymbol{c}$) Now ϕ only tracks interface ($0 \leq \phi \leq 1$)

Thermodynamic functional of Grand-potential $\Omega[\phi, \mu_c]$ **From M. Plapp, 2011**

$$\Omega[\phi, \boldsymbol{\mu}] = \int_V \Big[\underbrace{\omega_{int}(\phi, \nabla\phi)}_{\text{interface}} + \underbrace{\omega_{bulk}(\phi, \boldsymbol{\mu})}_{\text{thermodynamics}} \Big] dV \quad \text{with} \quad \begin{cases} \omega_{int}(\phi, \nabla\phi) & = H\phi^2(1-\phi)^2 + \frac{\zeta}{2}\left|\nabla\phi\right|^2 \\ \omega_{bulk}(\phi, \boldsymbol{\mu}) & = p(\phi)\omega_0(\boldsymbol{\mu}) + [1 - p(\phi)]\,\omega_1(\boldsymbol{\mu}) \\ p(\phi) & = \phi^2(3 - 2\phi) \end{cases}$$

$$\omega_\Phi(\boldsymbol{\mu}) = f_\Phi(\boldsymbol{c}) - \boldsymbol{\mu} \cdot \boldsymbol{c} \qquad \text{(Legendre transform)}$$

Assumption: quadratic free energies for f_Φ (2 parabolas)

$$f_\Phi(\boldsymbol{c}) = \frac{1}{2}\boldsymbol{K}_\Phi : (\boldsymbol{c} - \boldsymbol{c}_\Phi^{eq})^2 \qquad \text{where} \quad \boldsymbol{K}_\Phi = \begin{pmatrix} K_\Phi^{AA} & K_\Phi^{AB} \\ K_\Phi^{AB} & K_\Phi^{BB} \end{pmatrix} \quad \text{for } \Phi = 0, 1$$

→ Determine $K_\Phi^{\alpha\beta}$ coefficients from the thermo landscape (Calphad)

Using the Calphad results for math model

1. Pre-processing

- Transform elements to oxides + global eq
- Turn off the grid minim (hyp local eq)
- interpolate the non-converging local eq

2. Free energy landscape from Calphad

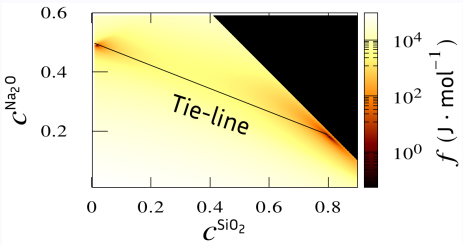

Methodology (1, 2, 3) from R. Le Tellier, 2021

3. Fit the tie-line with two parabolas

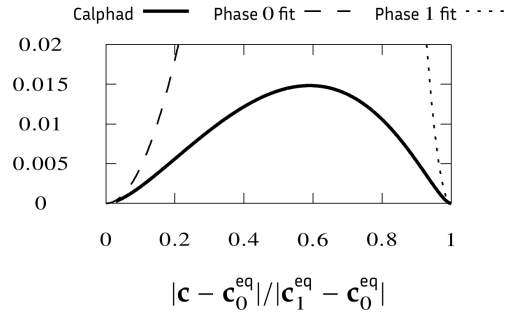

→ We obtain the $K_\Phi^{\alpha\beta}$ coefficients

Phase-field model to simulate

Thermodynamics: compositional Allen-Cahn (ϕ^{AC}-model)

Interface tracking

$$\frac{\partial \phi}{\partial t} + \overbrace{\boldsymbol{\nabla} \cdot (\boldsymbol{u}\phi)}^{\text{Advective term}} = M_\phi \overbrace{\left[\boldsymbol{\nabla}^2\phi - \frac{1}{4W^2}\omega'_{dw}(\phi)\right]}^{\text{Curvature } \kappa\left|\boldsymbol{\nabla}\phi\right|} - \overbrace{\frac{\lambda M_\phi}{W^2} p'(\phi)\left[\omega_0(\boldsymbol{\mu}) - \omega_1(\boldsymbol{\mu})\right]}^{\text{Thermodynamic}} \qquad (2)$$

Diffusion Eqs of SiO_2 and Na_2O

$$\frac{\partial c^A}{\partial t} + \boldsymbol{\nabla} \cdot (\boldsymbol{u} c^A) = \boldsymbol{\nabla} \cdot \left[D^A(\phi)\boldsymbol{\nabla}\mu^A\right] \qquad (3a)$$

$$\frac{\partial c^B}{\partial t} + \boldsymbol{\nabla} \cdot (\boldsymbol{u} c^B) = \boldsymbol{\nabla} \cdot \left[D^B(\phi)\boldsymbol{\nabla}\mu^B\right] \qquad (3b)$$

Relationship between $\boldsymbol{\mu}$ and $\boldsymbol{c}$

$$\boldsymbol{\mu} = \boldsymbol{K}(\phi)\left[\boldsymbol{c} - \boldsymbol{c}^{eq}(\phi)\right] \qquad (3c)$$

Initial conditions

using $\boldsymbol{c}_0^{eq}$, $\boldsymbol{c}_1^{eq}$ and $\boldsymbol{C}^{glass}$ (details in Part 3)

Illustration of ϕ^{AC}-model: Ostwald ripening

The phenomenon

Smaller droplets vanish whereas the larger ones grow because

- Larger droplets have a lower μ (Gibbs-Thomson cond)
- Diffusion flux from lower to larger droplets ($\boldsymbol{j} \propto -\boldsymbol{\nabla}\mu$)

→ Expected mean radius: $\langle R \rangle \propto t^{1/3}$ ↓

Simulation (from C. MÉJANÈS)

Video

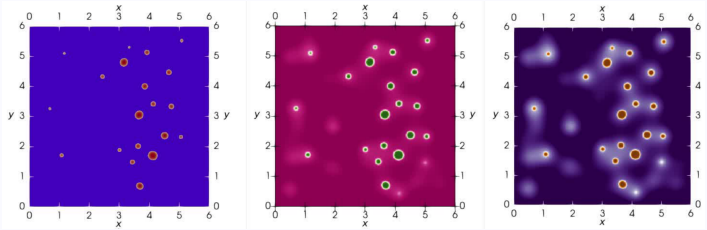

Verification

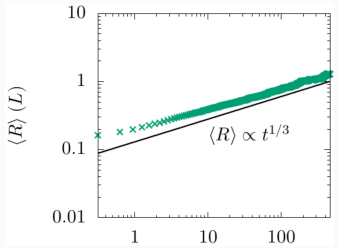

3D simulations of thermodynamics with fluid flow

Coupling with fluid flow

Hydrodynamics properties

- ρ_0, ρ_1: bulk **densities** of each phase

$$\varrho(\phi) = \rho_1\phi + \rho_0(1-\phi)$$

- η_0, η_1: **viscosities** of each phase

$$\eta(\phi) = \frac{\eta_0\eta_1}{\phi\eta_0 + (1-\phi)\eta_1}$$

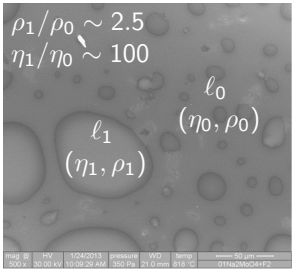

Navier-Stokes (NS) with gravity and capillary forces

$$\boldsymbol{\nabla} \cdot \boldsymbol{u} = 0 \tag{4a}$$

$$\frac{\partial \varrho \boldsymbol{u}}{\partial t} + \boldsymbol{\nabla} \cdot (\varrho \boldsymbol{u}\boldsymbol{u}) = -\boldsymbol{\nabla} p + \boldsymbol{\nabla} \cdot \left[\eta(\phi)\left(\boldsymbol{\nabla}\boldsymbol{u} + \boldsymbol{\nabla}\boldsymbol{u}^T\right)\right] + \underbrace{\mu_\phi \boldsymbol{\nabla}\phi}_{\text{Capillary force } \boldsymbol{F}_s} + \underbrace{\varrho \boldsymbol{g}}_{\text{Buoyancy}} \tag{4b}$$

$\boldsymbol{F}_s$ involves σ, κ, $\boldsymbol{n}$ ▸ Appendix

3D simulations with the HPC code LBM_Saclay

Main features of LBM_Saclay

- **Multi-architecture HPC**
  - multi-CPUs/GPUs
  - Kokkos (//intra-node - OpenMP/Cuda)
  - MPI (domain decomposition)
- 2D/3D **Lattice Boltzmann Methods** (LBM)

OpenSource: GitLab, licence CECILL

Documentation: Developpers' guide
GitLab, PhD and presentations

Programmers: P. Kestener, W. Verdier, T. Boutin, E. Stavropoulos, C. Méjanès, T. Duez, H. Keraudren, C. Elharti, A. Cartalade + interns M2

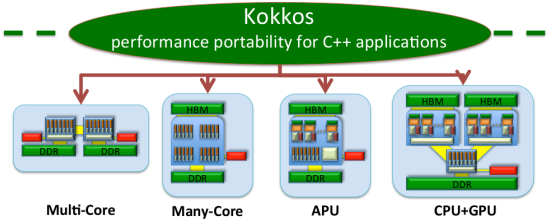

Jean-Zay (V100)

Topaze (A100)

List of verifications using ϕ^{AC}-model

Fluid-Fluid interface

Phenomena	Equations	LBM_Saclay	Who	Illustrations	Date
Diffusion couple	ϕ^{AC}+2C	☑	PhD Méjanès	**See poster**	2022
Double-Poiseuille Laplace law	ϕ^{AC}+NS	☑	PhD Méjanès	**See poster**	2022
Rayleigh-Taylor instab Splashing droplet	ϕ^{AC}+NS	☑	Théo Duez	**Next slide** Other pres	2023
Film boiling	ϕ^{AC}+NS+T	☑	PhD Verdier	Other pres	2020
Ostwald ripening	ϕ^{AC}+NS+2C	☑	PhD Verdier	**Next slide**	2022

Fluid-Solid interface

Phenomena	Equations	LBM_Saclay	Who	Illustrations	Date
Crystal growth	$\phi^{AC}+T+C$	☑	PhD Younsi		2015
Dissolution process	$\phi^{AC}+C$	☑	PhD Boutin	▸ Appendix	2021
Maturation of gels	$\phi^{AC}+2C$	☑	PhD Boutin	Other pres	2022

3D verification of two-phase flows

Classical test case of Rayleigh-Taylor instability

3D verification of NS + ϕ^{AC} eq

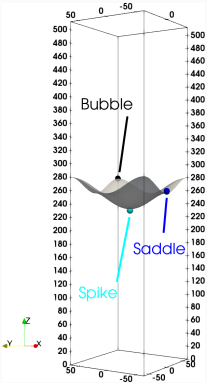

Mesh: ∼8.4M nodes

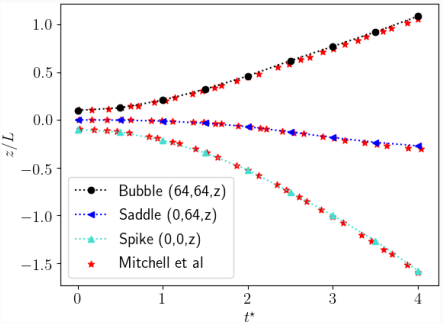

At = 0.5, Re = 128, Ca = 9.1, Pe = 744 ▸ Appendix

Simulation on Topaze-A100

Test case with

- ϱ and η contrast (ratio 3)
- gravity and surface tension

Mesh: 900×900×512 (∼415M nodes)

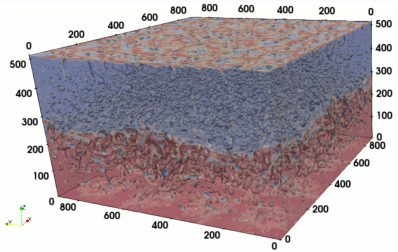

▸ Video 144 GPUs

Ostwald ripening with sedimentation

from W. Verdier (PhD, 2022)

Setup of simulation

- Initial conditions
  - For $\phi(\boldsymbol{x}, 0)$: $\sim$2000 droplets of radius $\langle R \rangle$
  - For $c(\boldsymbol{x}, 0)$
    - Supersaturation imposed in the matrix
    - Equilibrium in the droplets

$$\boldsymbol{c}(\boldsymbol{x}, 0) = \begin{cases} (1-\delta)\boldsymbol{c}_0^{eq} + \delta \boldsymbol{c}_1^{eq} & \text{if } \phi < 1/2 \\ \boldsymbol{c}_1^{eq} & \text{if } \phi \geq 1/2 \end{cases}$$

$$\text{with} \quad \delta = \frac{s^{eq} - s^{ini}}{1 - s^{ini}}, \; s^{eq} = \frac{\left|\boldsymbol{c}_0^{eq} - \boldsymbol{C}^{glass}\right|}{\left|\boldsymbol{c}_0^{eq} - \boldsymbol{c}_1^{eq}\right|}$$

- Gravity + capillary forces

Simulation on Topaze-A100

Mesh 2048×512×512 nodes

2.368.000 time-iter

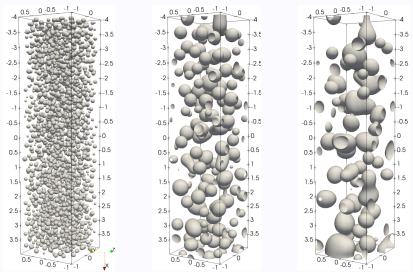

$t(\times 10^5) = 0$ | 3.68 | 10.72

▸ Video 64 GPUs

Diffusion effect

Characteristic times

- Diffusion

$$t_{diff} = \frac{L}{2D}$$

- Flow

$$t_{flow} = \sqrt{\frac{L}{2g}}$$

  - L is the domain width
  - D diffusion coeff
  - g gravity

Comparison

At $t = 1.000.000$ time-iter

D | $D/100$

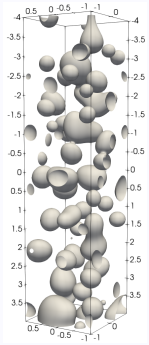

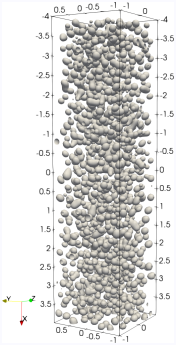

$t_{diff} \simeq t_{flow}$ | $t_{flow} \ll t_{diff}$

What next ?

Experimental device (LDPV): furnace + camera

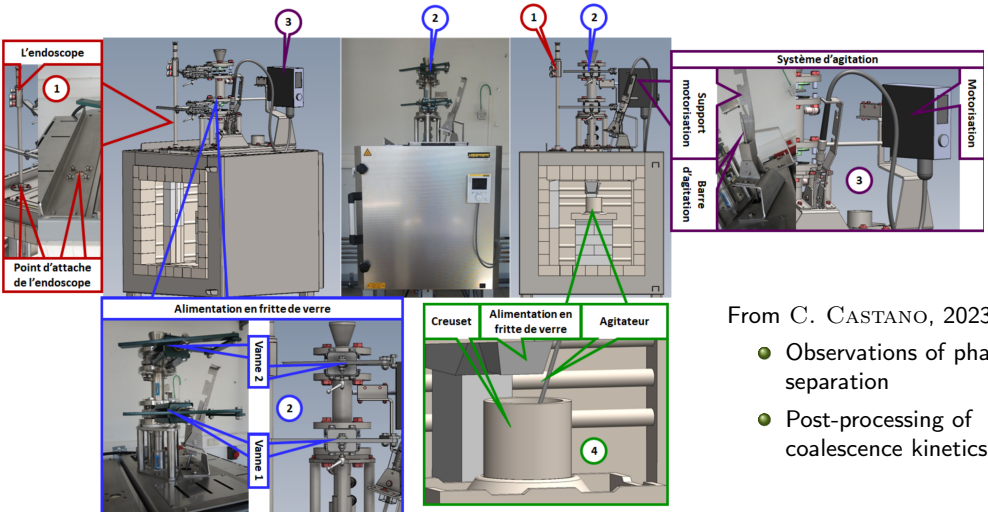

From C. Castano, 2023

- Observations of phase separation
- Post-processing of coalescence kinetics

Work in progress and perspectives

Work In progress

1. Mathematical model improvement
   - Add the thermo of SiO_2–Na_2O–MoO_3–B_2O_3 (quaternary)
   - Add a new transport equation in `LBM_Saclay`
2. Experiments
   - Observations and measures for ternary glass
   - Data post-processing for coalescence kinetics

Perspectives: converge both

More general perspectives for ϕ-model

- Introduce the chemical reactions
- Extend to "three-phase/multi-components" ▸ Video

Thank you for watching

APPENDICES

Pros and cons of using phase-field modeling

Return

Pros

1. A unique eulerian mesh is used for tracking the interface
2. Can simulate complex topologies (spinodal decomposition, crystal growth, ...)
3. Coalescence can be simulated without additional model
4. Possible generalization for multi-phase and multi-components

Cons

1. Diffuse interface width W, coupling param λ, and surface tension σ
2. Requires many parameters $(c_{\ell_0}^{eq}, c_{\ell_1}^{eq}, \overline{\mu}^{eq}, D_{\ell_0}, D_{\ell_1}, \eta_{\ell_0}, \eta_{\ell_1}, \rho_{\ell_0}, \rho_{\ell_1})$ and more for multi-components
3. The PDEs can be complex and their physical meaning are lost
4. Require performing "asymptotic expansions"

Computational times on GPU vs CPU

P. Kestener (2018)

3D transport (without MPI)

Perfs on 3 graphics cards (K80, P100 and V100)

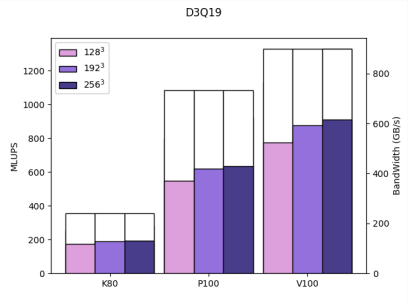

GPU

Perfs on 2 optimisations CSoA and CSoA2 on Intel KNL (CSoA = Cluster of Structure of Array)

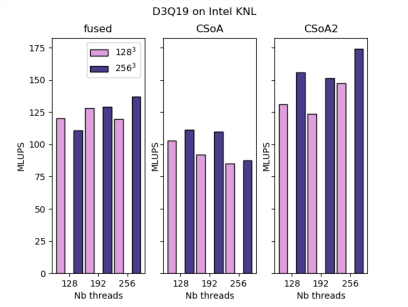

CPU KNL (TGCC Irene)

Euler-Lagrange equation and chemical potential

Minimization of functional (see principle of least action)

$$\mathscr{F}[\phi] = \int_V \mathcal{F}(\phi, \boldsymbol{\nabla}\phi) dV \tag{5}$$

↓ Application of δ operator (variational derivative)

$$\delta\mathscr{F}[\phi] = \int_V \Big[\frac{\partial \mathcal{F}}{\partial \phi} - \underbrace{\partial_\alpha \left(\frac{\partial \mathcal{F}}{\partial(\partial_\alpha \phi)}\right)}_{\text{Einstein convention}}\Big]\delta\phi dV = 0 \tag{6}$$

We obtain the Euler-Lagrange equation:

$$\boxed{\frac{\partial \mathcal{F}}{\partial \phi} - \boldsymbol{\nabla}\cdot\left(\frac{\partial \mathcal{F}}{\partial(\boldsymbol{\nabla}\phi)}\right) = 0} \tag{7}$$

Application

$$\mathcal{F} = H\underbrace{\phi^2(1-\phi)^2}_{g_1(\phi)} + \tfrac{\zeta}{2}(\boldsymbol{\nabla}\phi)^2$$

↓ (Euler-Lagrange eq.)

$$Hg_1'(\phi) - \zeta\boldsymbol{\nabla}\cdot(\boldsymbol{\nabla}\phi) = 0$$

g_1' derivative wrt ϕ

Chemical potential $\mu_\phi = \delta\mathcal{F}/\delta\phi$

Conjugate variable (intensive) of composition (extensive)

$$\mu_\phi = \frac{\partial \mathcal{F}}{\partial \phi} - \boldsymbol{\nabla}\cdot\left(\frac{\partial \mathcal{F}}{\partial(\boldsymbol{\nabla}\phi)}\right)$$
$$= Hg_1'(\phi) - \zeta\boldsymbol{\nabla}^2\phi$$

Alternative forms of double-wells

Return

For $g_1(\phi)$ the two minima are $\phi_A = 0$, $\phi_B = 1$ and $g_1(\phi_A) = g_1(\phi_B) = 0$

Modification of minima ϕ_A and ϕ_B

Function $g_2(\phi) = (\phi - \phi_A)^2(\phi - \phi_B)^2$

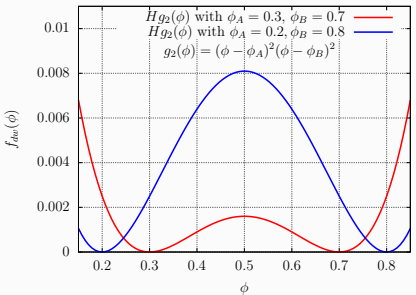

Modification of height

Function $g_1(\phi)$ and $p(\phi) = \phi^3(10 - 15\phi + 6\phi^2)$

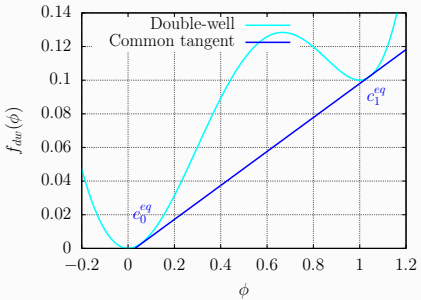

Special case $\phi_A = +\phi^\star$ and $\phi_B = -\phi^\star$

$$g(\phi) = (\phi - \phi^\star)^2(\phi + \phi^\star)^2$$

Properties of interpolation function $p(\phi)$

$$p(0) = 0,\ p(1) = 1 \quad \text{and} \quad p'(0) = p'(1) = 0$$

Thermodynamics of binary mixtures

Return

Binary phase diagram

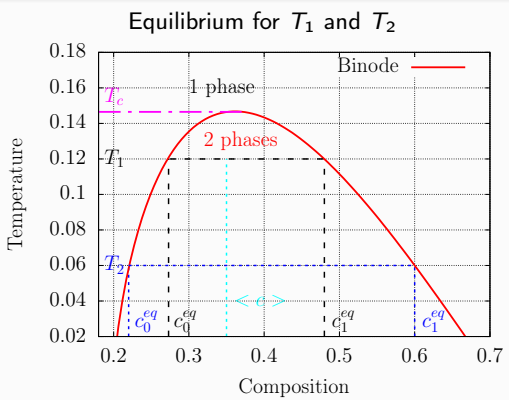

Corresponding double-wells

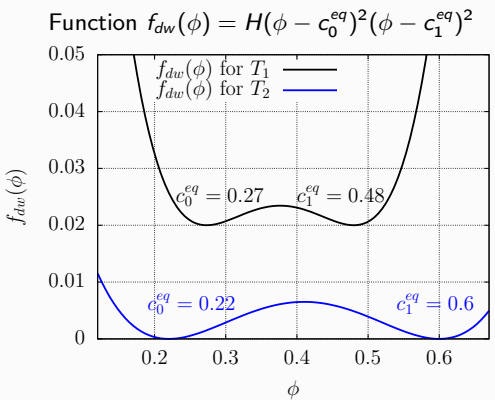

Interpretation of the capillary force

Return

From Brackbill *et al*, JCP (1992) & Jacqmin JCP (1999)

F_s contains σ and κ and $n = \nabla\phi/|\nabla\phi|$

$$\boldsymbol{F_s} = \mu_\phi \boldsymbol{\nabla}\phi = -\delta_d \sigma \kappa \boldsymbol{n}$$

Demo using Eq. for μ_ϕ

$$\begin{aligned}
\boldsymbol{F_s} = \mu_\phi \boldsymbol{\nabla}\phi &= \Big[4 \underbrace{H}_{\text{Eq. (9)}} \phi(\phi-1)(\phi-1/2) - \underbrace{\zeta}_{\text{Eq. (8)}} \nabla^2\phi\Big]\boldsymbol{\nabla}\phi \\
&= -\frac{3}{2} W\sigma \underbrace{\left[\Delta\phi - \frac{16}{W^2}\phi(1-\phi)(1-2\phi)\right]}_{\kappa|\nabla\phi| \text{ Eq (10)}} \boldsymbol{\nabla}\phi \\
&= -\frac{3}{2} W\sigma\kappa\,|\nabla\phi|\,\boldsymbol{\nabla}\phi \\
&= -\delta_d \sigma\kappa \boldsymbol{n} \qquad \text{with } \delta_d = \frac{3}{2} W\,|\nabla\phi|^2
\end{aligned}$$

We can check that

$$\zeta = \frac{3}{2} W\sigma \tag{8}$$

$$H = 12\frac{\sigma}{W} \tag{9}$$

Curvature term

$$\begin{aligned}
\kappa\,|\nabla\phi| &= (\nabla\cdot\boldsymbol{n})\,|\nabla\phi| \\
&= \nabla\cdot(|\nabla\phi|\,\boldsymbol{n}) - \boldsymbol{n}\cdot\nabla\,|\nabla\phi| \\
&= \nabla\cdot\left(\cancel{|\nabla\phi|}\frac{\nabla\phi}{\cancel{|\nabla\phi|}}\right) - \boldsymbol{n}\cdot\nabla\,|\nabla\phi| \\
&= \nabla^2\phi - \frac{16}{W^2}\phi(1-\phi)(1-2\phi) \qquad (10)
\end{aligned}$$

Initial conditions of Cahn-Hilliard model

Return

Initial conditions: r random number (uniform distrib): $0 \leq r \leq 1$

- **Nucleation-growth**

$$\phi(\boldsymbol{x}, 0) = \begin{cases} 0.2 & \text{for 97\% of nodes} \\ \frac{(9+r)}{10} & \text{for 3\%} \end{cases}$$

- **Spinodal decomposition**

$$\phi(\boldsymbol{x}, 0) = r, \quad \text{for all nodes}$$

- **Demixing**

$$\phi(\boldsymbol{x}, 0) = \begin{cases} \frac{3}{10} r & \text{for 90\% of nodes} \\ \frac{9+r}{10} & \text{for 10\%} \end{cases}$$

The positions of 10% nodes $\boldsymbol{x}_g = (x_g, y_g)$ follow a gaussian distribution

Simulations of spinodal decomposition

Return

Standard spinodal decomposition

Cahn-Hilliard Eq.

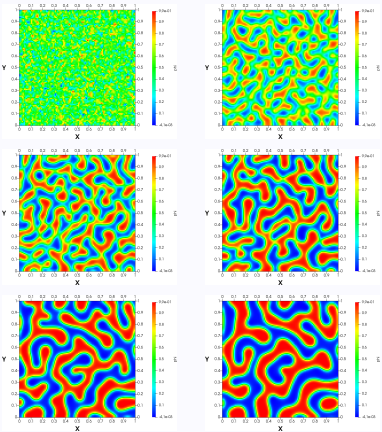

Spinodal decomposition with surfactant

Cahn-Hilliard Eq.

$t_0 = 0$ $t_1 = 10\delta t$ $t_2 = 10^3\delta t$

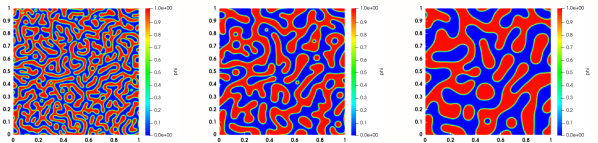

Composition Eq.

$t_0 = 0$ $t_1 = 10\delta t$ $t_2 = 10^3\delta t$

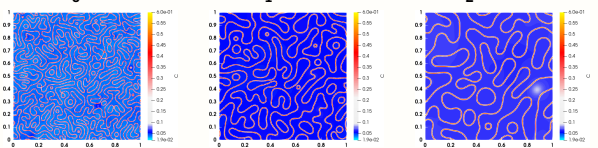

From H. de Gieter (LMSF, 2022) Video

«ϕ-models+LBM» 1/2: PhD (part a)

PhD A. Younsi: crystal growth

2012–2015

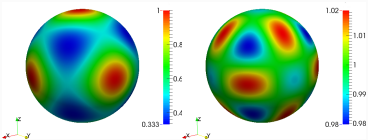

Anisotropy functions

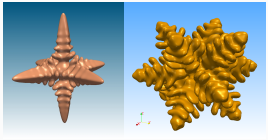

Effects on crystal growth

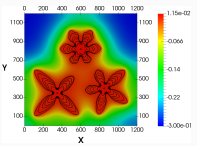

Interaction of crystals

PhD W. Verdier: Ostwald ripening with fluid flow

2019–2022

- Liquid-Liquid, three components
- Ostwald ripening with fluid flow

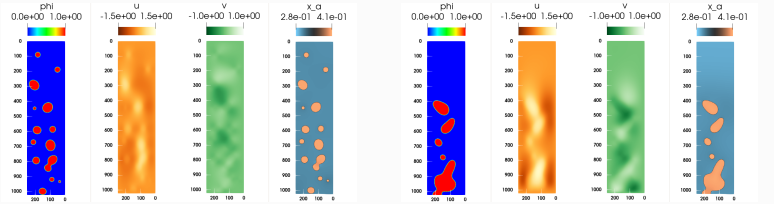

Ostwald ripening with fluid flow

PhD T. Boutin: maturation of gels (solid/liquid), SiO_2–B_2O_3–water

2021–2024

Without curvature effect

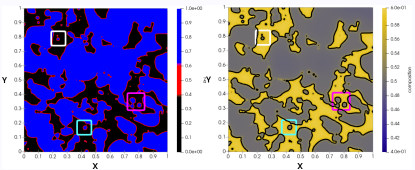

C homogeneous in solid

With curvature effect

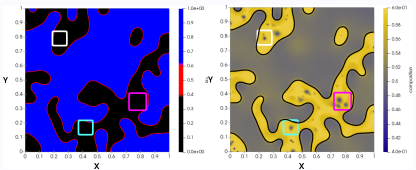

C heterogeneous in solid

PhD C. Méjanès: ternary demixing SiO_2–Na_2O–MoO_3 (liquid/liquid)

2022–2025

- Interface between **math model** and **experiments** of CEA/Marcoule
- Improve the link with the thermo of SiO_2–Na_2O–MoO_3
- **Predictive simulations** of two-phase ternary glasses

Verifications LBM_Saclay: dissolution

Return

Analytical solutions

Compositions c_s and c_l

$$c_s^{as}(x,\ t) = c_s^{\infty} + (c_s^{co} - c_s^{\infty})\frac{\text{erfc}\left[-x/2\sqrt{D_s t}\right]}{\text{erfc}\left[-\alpha/2\sqrt{D_s}\right]}$$

$$c_l^{as}(x,\ t) = c_l^{\infty} + (c_l^{co} - c_l^{\infty})\frac{\text{erfc}\left[x/2\sqrt{D_l t}\right]}{\text{erfc}\left[\alpha/2\sqrt{D_l}\right]}$$

Interface position

$$x_i(t) = \alpha\sqrt{t}$$

with α computed with transcendental eq:

$$\alpha = 0.184841$$

Parameters

$D_s = 0.9$ $\quad m_s = 0.2$

$D_l = 1$ $\quad m_l = 0.1$

$c_s^{\infty} = 0.75$ $\quad \Delta m = 0.1$

$c_l^{\infty} = 0.4$ $\quad \Delta \overline{f}^{min} = 0.04$

All details and other validation in doi

Comparisons with LBM_saclay

Compositions c_s and c_l

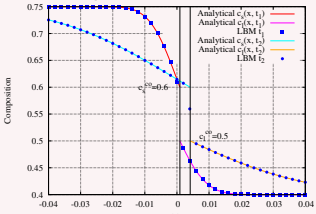

Interface position

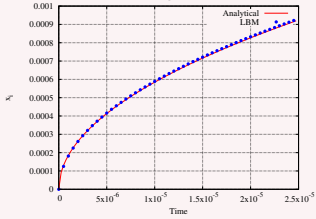

Dimensionless numbers for RT instability

Return

For Rayleigh-Taylor

Velocity U_0

$$U_0 = \sqrt{gL}$$

Atwood number

$$\mathrm{At} = \frac{\rho_h - \rho_l}{\rho_h + \rho_l}$$

Nomenclature 1/2

- L: domain width
- g: gravity
- $\rho_{h,l}$: densities heavy and light

For fluid flow

Reynolds number

$$\mathrm{Re} = \frac{U_0 L}{\nu}$$

Capillary number

$$\mathrm{Ca} = \frac{\eta_h U_0}{\sigma}$$

Bond or Eötvös

$$\mathrm{Bo} = \frac{\Delta\rho g L^2}{\sigma}$$

For interface tracking

Peclet number

$$\mathrm{Pe}_\phi = \frac{U_0 L}{M_\phi}$$

Nomenclature 2/2

- ν, η kinematic and dynamic viscosities
- σ: surface tension
- $\Delta\rho$: density diff
- M_ϕ: interface mobility

Conclusion and perspectives: towards 3 phases

Return

Nomenclature : ^{NS}=Navier-Stokes ^{CH}=Cahn-Hilliard ^{AC}=Allen-Cahn ^{CAC}=Conservative Allen-Cahn

Phenomenology	Taken into account via						Currently neglected
1 phase	T	C	NS	ϕ	Nb comp	Examples	
☑ Thermics advective & diffusive	☑	☐	☐				Radiation
☑ Transport advective & diffusive	☐	☑	☐				≥ 4 components
☑ Flows (incomp, lamin, viscous)	☐	☐	☑				Non-newtonian fluids
2 phases						Fluid - Interf - Solid	
☑ Phase change (liquid/solid)	☑	☑	☑	AC	2	Crystal growth	Big Lewis nb
☑ Dissolution/precipitation	☐	☑	☑	AC	3	Dissolution solid phase	NS coupling
☑ Interface adsorption	☐	☑	☑	AC		Porous media retention	To be done
						Fluid1 - Interf - Fluid2	
☑ Demixing (phase separation)	☑	☑	☑	CH	2	Spinodal decomp	T coupling
☑ Coalescence & break-up	☑	☑	☑	CH	2	Rising bubbles	T coupling
☑ Instabilities	☑	☑	☑	CAC	2	Rayleigh-Taylor	T coupling
☑ Phase change (liquid/gas)	☑	☑	☑	CAC	1	Film boiling	Big density ratios
☑ Exchange through interface	☑	☑	☑	AC	3	Ostwald ripening	T coupling
☑ Interface adsorption	☐	☑	☑	CH	1	Surfactant	NS Coupling
3 phases and more							
☑ 2 immisc fluids + solid	☐	☐	☐			2 liquids + SiO_2	To explore
						Unsaturated porous media	
☑ 3 immisc fluids	☐	☑	☑			3 liquids	In progress